Remote Sensing of Environment 139 (2013) 246–256

Contents lists available at ScienceDirect

Remote Sensing of Environment

journal homepage: www.elsevier.com/locate/rse

Methane concentrations over Monsoon Asia as observed by SCIAMACHY: Signals of methane emission from rice cultivation

S. Hayashida [a,*], A. Ono [a], S. Yoshizaki [a,1], C. Frankenberg [b], W. Takeuchi [c], X. Yan [d]

[a] Faculty of Science, Nara Women's University, Kitauoya Nishimachi, Nara 630-8506, Japan
[b] Jet Propulsion Laboratory, 4800 Oak Grove Drive, Pasadena, CA 91109, USA
[c] Institute of Industrial Science, University of Tokyo, 6-1, Komaba 4-chome, Meguro, Tokyo 153-8505, Japan
[d] State Key Laboratory of Soil and Sustainable Agriculture, Institute of Soil Science, Chinese Academy of Sciences, Nanjing, China

ARTICLE INFO

Article history:
Received 11 January 2013
Received in revised form 2 August 2013
Accepted 3 August 2013
Available online 4 September 2013

Keywords:
Methane
SCIAMACHY
Monsoon Asia
Rice paddies
Atmosphere

ABSTRACT

We have analyzed the column-averaged CH_4 concentration (xCH_4) using scanning imaging absorption spectrometer for atmospheric chartography (SCIAMACHY) and compared the data with the bottom–up emission inventory data sets and other satellite-derived indices such as the land-surface water coverage (LSWC) and the normalized difference vegetation index (NDVI). The geographical distribution of high CH_4 values corresponds to strong emissions from regions where rice is cultivated, as indicated in the inventory maps. The Pearson's correlation coefficients (r) between xCH_4 and the rice emission inventory data are observed to be greater than ~0.6 over typical rice fields, with outstanding r-values of ~0.8 in the Ganges Basin, Myanmar, and Thailand. This suggests that the emission of CH_4 from rice cultivation mainly controls the seasonality of the CH_4 concentration over such regions. The correlation between xCH_4 and LSWC and NDVI is also as large as 0.6. In Southeast Asia, the r-values of xCH_4 with bottom–up inventory data that includes all categories are not as high as those with the emission, as estimated from the rice category only. This is indicative of the relative importance of rice emissions among all other emission categories in Southeast Asia.

1. Introduction

The concentration of atmospheric methane (CH_4) has more than doubled since pre-industrial times, and its radiative forcing is estimated to be the second largest after carbon dioxide (CO_2) (Forster et al., 2007). However, despite the importance of atmospheric CH_4 in global warming, the significance of individual sources of CH_4 remains highly uncertain (e.g., Dlugokencky, Nisbet, Fisher, & Lowry, 2011).

Many observations were performed to improve our understanding of the various CH_4 sources (e.g., Dlugokencky, Lang, & Masarie, 2009; Dlugokencky, Bruhwiler, et al., 2009). The world meteorological organization's (WMO) global atmosphere watch (GAW) program has taken the initiative of monitoring of atmospheric CH_4 across the world. The data obtained at GAW monitoring stations are made available to the public through The World Data Centre for Greenhouse Gases (WDCGG). Though the current observational network can provide plenty of data to constrain emissions on a global scale, their coverage is insufficient to determine emissions on a regional scale. In addition, most of the current observational sites monitor the background levels of CH_4 concentrations only. Ground-based observation stations are still sparsely distributed in some important source regions, such as the inland areas of Asia and most of Siberia.

Among the various approaches available for measuring the CH_4 concentration, satellite observations have the advantage of providing continuous monitoring of atmospheric species over a wide spatial range, thereby enabling the analysis of spatial and temporal variations with a reasonable resolution. The scanning imaging absorption spectrometer for atmospheric chartography (SCIAMACHY) onboard the ENVISAT satellite allowed the first global measurements of atmospheric CH_4 from space (Frankenberg, Meirink, van Weele, Platt, & Wagner, 2005; Frankenberg et al., 2006), and the derived data have been used in many scientific studies. The global maps of CH_4 generated using the SCIAMACHY reveal that CH_4 emission over Monsoon Asia is noticeably high. Monsoon Asia accommodates about 90% of the world's rice fields and a large number of domestic ruminants (e.g., FAO, 2013).

The SCIAMACHY measures the spectra of the solar reflectance at short-wavelength of the infrared (SWIR), its measurement provides the information of CH_4 distribution at lower altitude down to the surface, while other thermal infrared (TIR) sensors generate information of CH_4 distribution at only mid- or upper-troposphere. As indicated by Randel et al. (2010), convection over the Monsoon Asia is so strong that condensed CH_4 plumes were sometimes observed in the upper troposphere. This was independently inferred from both the TIR satellite sensor (Xiong et al., 2009), as well as from airborne measurements (Baker et al., 2012). Such studies have brought a new aspect of CH_4

* Corresponding author. Tel.: +81 742203440; fax: +81 742203441.
E-mail address: sachiko@ics.nara-wu.ac.jp (S. Hayashida).
[1] Now at: NTT DATA Co. Ltd., Tokyo 135-6033, Japan.

0034-4257/$ – see front matter © 2013 Elsevier Inc. All rights reserved.
http://dx.doi.org/10.1016/j.rse.2013.08.008

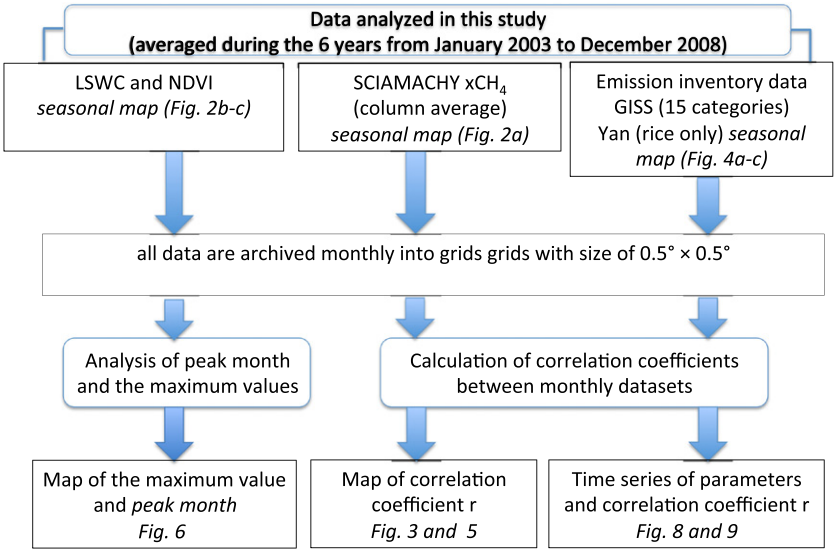

Fig. 1. A flow chart of the data processing technique applied in this study.

emission estimation coupled with the atmospheric transport model. However, the CH_4 concentration in the lower troposphere should be more influenced by the CH_4 emission from the ground; and thus, the data obtained from SWIR sensors are more indicative of the emissions from the ground. Sheshakumar, Singh, Panigrahy, and Parihar (2011) indicated that the CH_4 concentration patterns match very closely with the growth patterns of rice in North India. In this study, we have also observed a similar relationship of high CH_4 concentration in rice cultivation areas over Monsoon Asia.

According to the research on bottom–up inventory databases such as NASA's Goddard institute for space studies (GISS) (Matthews, Fung, & Lerner, 1991), Asia contributes about 155 Tg of CH_4 emissions annually, which represents more than one-fourth of the total global emission (Denman et al., 2007). As per the GISS estimates, among all individual source categories, rice cultivation contributes the maximum amount of CH_4 emission in Monsoon Asia. However, significant uncertainty remains in the quantitative estimation of CH_4 emissions from rice cultivation. The intergovernmental panel on climate change (IPCC, 1994) summarized the scattered values in their early studies, estimating a mean of 60 Tg CH_4 yr^{-1} with a range of 20–100 Tg CH_4 yr^{-1}. The most recent bottom–up study by Yan, Akiyama, Yagi, and Akimoto (2009) (referred to as YAN2009 hereafter), who applied the Tier 1 model recommended by the IPCC (IPCC, 2007), estimated global CH_4 emission from rice fields in 2000 to be 25.6 Tg yr^{-1}. Their estimate is at the lower end of the range estimated by IPCC (see Fig. 1 of YAN2009).

To reduce the uncertainty in CH_4 emission on a regional scale, we need to examine the changes in the geographical distribution of CH_4 in more detail, including seasonal and year-to-year variability, and to compare these findings with factors that control CH_4 emission. As suggested by Sass and Cicerone (2002), methane emission from rice fields is the result of complex processes including anaerobic fermentation of carbon sources such as straw and additional fertilizers. Water flooding of rice fields creates an anaerobic environment that promotes such processes. Rice plants play a crucial role in methane emission from rice paddies as well. First, rice roots are a source of carbon and oxygen that affect the production and oxidation of methane. Second, the majority of methane emission from rice paddies is transported through rice plants (Cicerone & Shetter, 1981; Seiler, Holzapfel-Pschorn, Conrad, & Scharffe, 1984). Therefore, factors such as water surface coverage and vegetation enhancement that corresponds to growth of rice should be closely related to CH_4 emission from rice paddy fields.

In this study, we have focused our attention only on Monsoon Asia and have shown the characteristics of the CH_4 distribution in this region. We have also determined the relationship between the atmospheric CH_4 concentration and other related factors; we have also compared the distribution of CH_4 using the SCIAMACHY CH_4 products with some satellite-derived indices to characterize surface conditions such as land-surface water coverage (LWSC) and normalized difference vegetation index (NDVI). Fig. 1 summarizes the data processing procedure applied in this study. The details of the data used in this study will be described in the following sections; SCIAMACHY CH_4 data will be described in Section 2, the LSWC and the NDVI in Section 3. For comparison, we will also use the emission inventory data, which will be described in Section 4. Distribution and correlation among those parameters mentioned above will be shown and discussed in Section 5.

2. Scanning imaging absorption spectrometer for atmospheric chartography (SCIAMACHY)

The SCIAMACHY instrument onboard the European space agency's environmental research satellite, ENVISAT, is an eight-channel grating spectrometer that takes measurements in the ultraviolet, visible, and near-infrared wavelengths (240–2380 nm) (Bovensmann et al., 1999). The satellite operates in a near-polar, sun-synchronous orbit at an altitude

Table 1
List of methane data and satellite-derived indices shown in Fig. 2.

	Satellite	Sensor	Grid size archived in this study	Reference
xCH_4	ENVISAT	SCIAMACHY	0.5° × 0.5°	Algorithm Version 5.5 Frankenberg et al. (2006)
Land Surface Water Coverage (LSWC)	Terra/Aqua Aqua	MODIS AMSER-E	0.5° × 0.5°[a]	Takeuchi and Gonzalez (2009)
Normalized Difference Vegetation Index (NDVI)	Terra/Aqua	MODIS	1° × 1°	Huete et al. (2002)

[a] 1/12° × 1/12° in the original data set.

Table 2
List of CH_4 emission estimates from bottom–up inventories shown in Fig. 4.

Database	Emission category	Grid archived	Reference
(a) GISS	All	1° × 1°	Matthews et al. (1991)
(b) GISS	Rice fields	1° × 1°	Matthews et al. (1991)
(c) Yan2009	Rice fields	0.5° × 0.5°	Yan et al. (2009)

of 800 km, with a local equator-crossing time of approximately 10:00 am. In the nadir mode, a swath of 960 km gives full global coverage every 6 days (14 orbits per day). The typical ground-pixel size of SCIAMACHY is 30 km along-track (approximately north–south) × 60–120 km across-track (approximately east–west). The CH_4 data are retrieved from the nadir spectra in a micro-window of Channel 6 ranging from 1640 to 1670 nm. A recent reanalysis of CH_4 spectroscopic parameters in this spectral range (Frankenberg et al., 2008) already resolved a potential retrieval bias due to erroneous pressure-broadening coefficients. Details of the retrieval method have been reported by Frankenberg et al. (2011). We used the product version 5.5 (IMAP v5.5) during the period from January 2003 through December 2008. For the analysis of time series (shown in Fig. 8), we added the data from January to March in 2009, though the 3 months data have not been included in other analyses.

As described by Frankenberg et al. (2006), the SCIAMACHY retrieval, the iterative maximum a posteriori differential optical absorption spectroscopy (IMAP-DOAS), uses CO_2 as a proxy to determine the air-mass factor. First, the total columns of CH_4 ($VCD(CH_4)$) and CO_2 ($VCD(CO_2)$) are retrieved from the observed spectra (Channel 6), and then, the volume mixing ratio of CO_2 ($VMR(CO_2)$) obtained from the model field calculated by CarbonTracker (Peters et al., 2007) is scaled by the ratio $VCD(CH_4)/VCD(CO_2)$ as:

$$VMR(CH_4) = \frac{VCD(CH_4)}{VCD(CO_2)} \times VMR(CO_2). \quad (1)$$

Here, $VMR(CH_4)$ is the column-averaged dry air mole fraction of atmospheric CH_4, which is indicated as xCH_4 hereafter.

The SCIAMACHY xCH_4 data obtained by daily swath measurements are arranged into grids of 0.5° × 0.5° in latitude and longitude, and are averaged monthly or seasonally. They are then compared with the indices described in Section 3.

3. Satellite-derived indices for comparison with SCIAMACHY xCH_4

We compared SCIAMACHY xCH_4 with LSWC and NDVI. Table 1 summarizes those indices analyzed in this study. The period analyzed in this study is from 2003 through 2009, in accordance with the version 5.5 of SCIAMACHY CH_4 data set. The details of these indices are described in the following subsections.

3.1. Land-surface water coverage (LSWC)

The LSWC was derived by Takeuchi and Gonzalez (2009); it provides the fraction of a land surface covered by water. The LSWC was

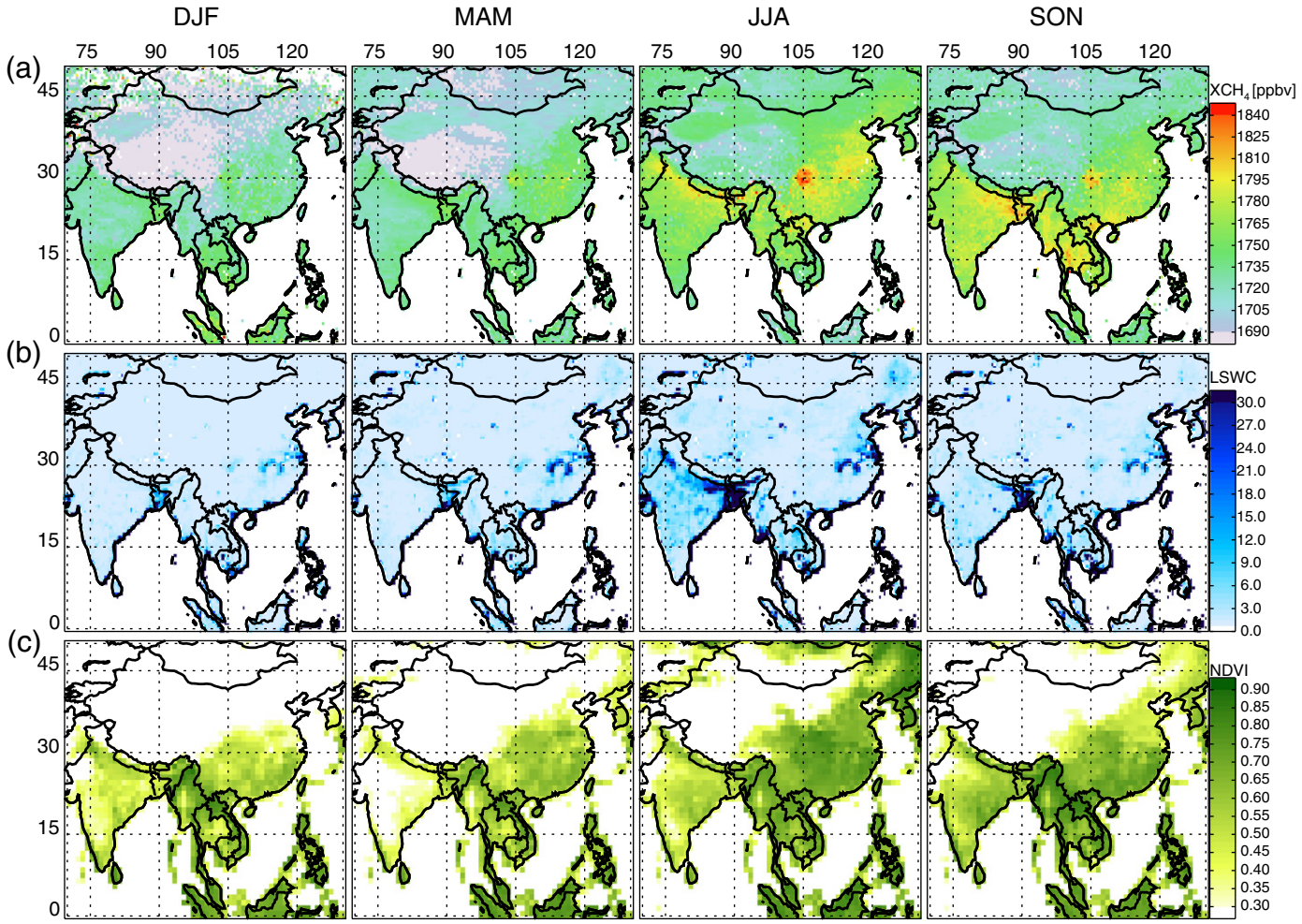

Fig. 2. Maps of 3-month average values of (a) SCIAMACHY xCH_4, (b) land-surface water coverage (LSWC), and (c) normalized difference vegetation index (NDVI). All data have been averaged for 6 years from January 2003 through December 2008. The columns correspond to DJF, MAM, JJA, and SON, respectively.

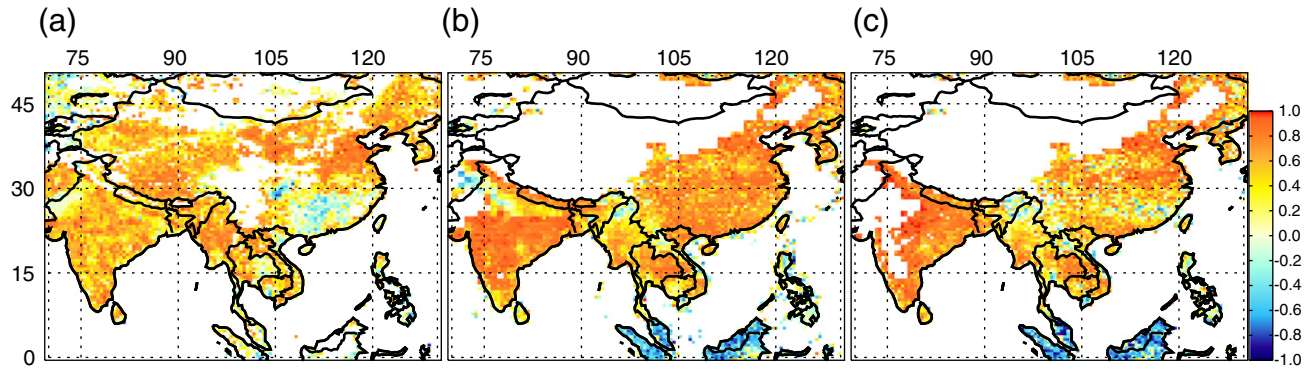

Fig. 3. The Pearson's correlation coefficients between SCIAMACHY xCH_4 and (a) LSWC and (b) NDVI. The number of matching pairs is more than six, for each grid, for the twelve months from January to December. (c) Same as in (b) but for the limited period from May to November.

derived by the combined use of moderate resolution imaging spectrometer (MODIS) onboard the Terra/Aqua and the advanced microwave scanning radiometer-EOS (AMSR-E) onboard the Aqua. The MODIS 8-day composite data with a 2-km resolution gives the normalized difference water index (NDWI); whereas, the AMSR-E daily data with a 16-km resolution gives the normalized difference polarization index (NDPI). Both these indices were used to produce a map of LSWC. The original data of LSWC are archived into grids of size 1/12° × 1/12° in latitude and longitude. In this study, we have averaged the data into a monthly 0.5° × 0.5° grid for comparing it with the other indices.

3.2. Normalized difference vegetation index (NDVI)

The NDVI is a well-known index for inferring the vegetation state, which is simply defined as follows:

$$\mathrm{NDVI} = (\mathrm{NIR} - \mathrm{VIS})/(\mathrm{NIR} + \mathrm{VIS}) \quad (2)$$

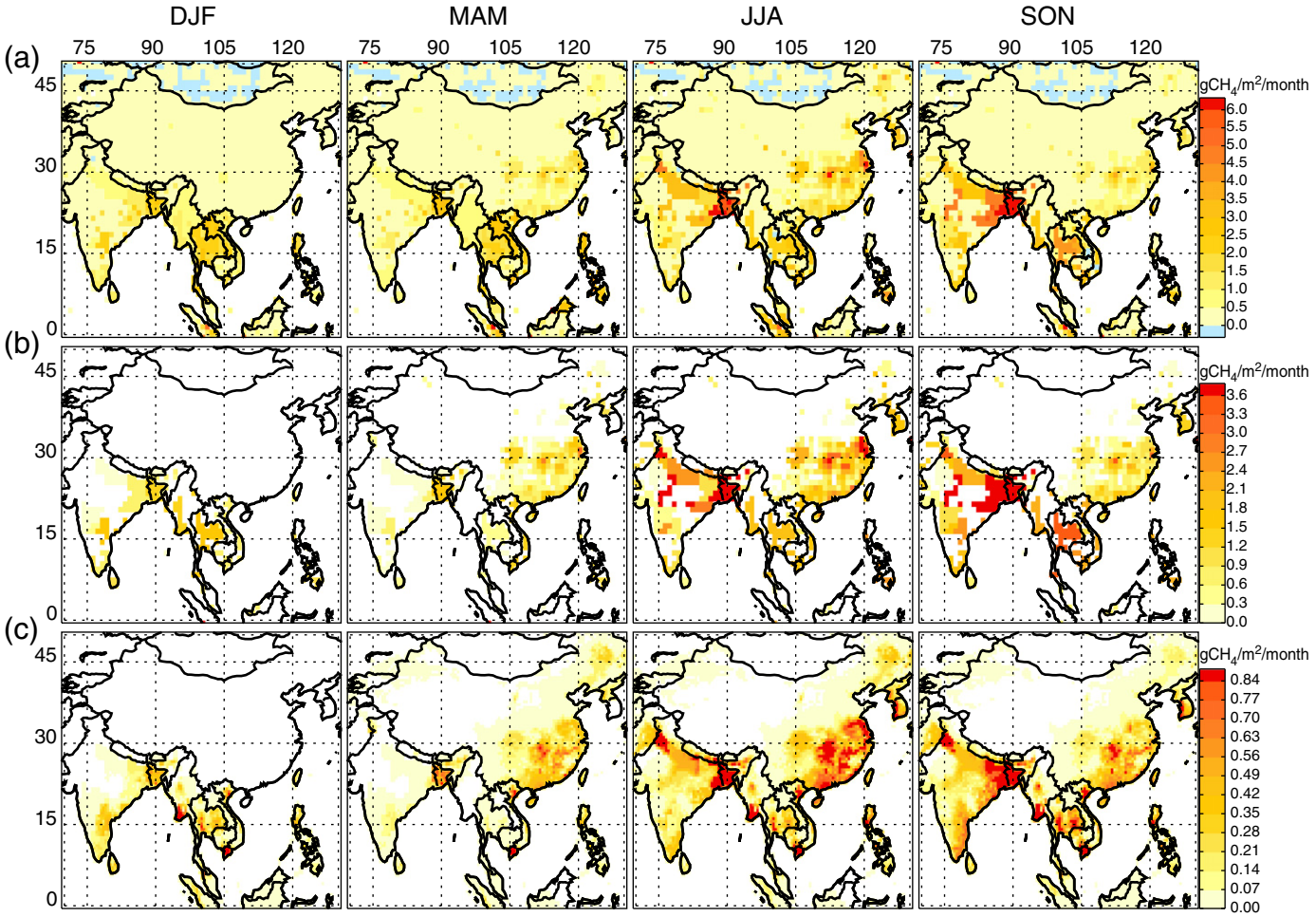

Fig. 4. Maps of 3-month averaged values of (a) GISS CH_4 emission flux estimates for all source categories, (b) GISS CH_4 emission flux estimate for rice cultivation, and (c) CH_4 emission flux by Yan et al. (2009). The columns correspond to DJF, MAM, JJA, and SON, respectively.

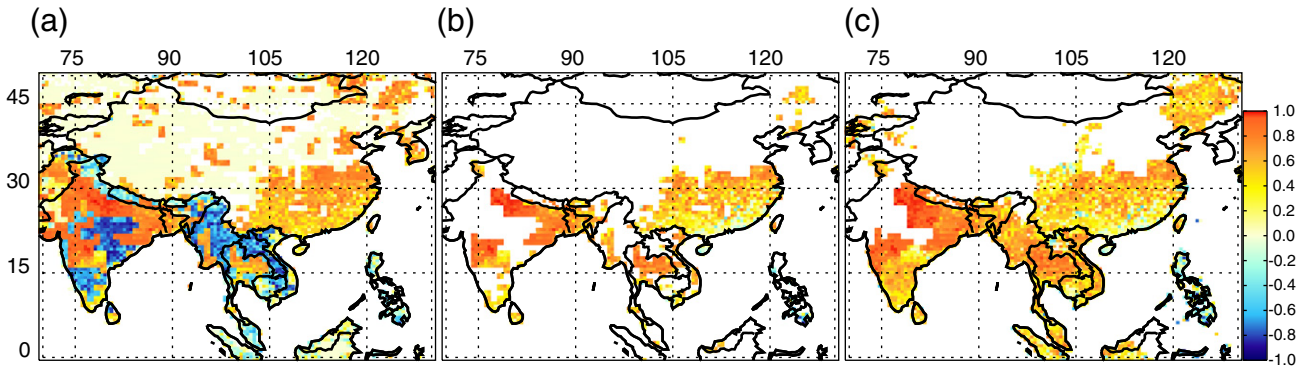

Fig. 5. The Pearson's correlation coefficients between SCIAMACHY xCH_4 and (a) GISS CH_4 estimates including all categories, (b) GISS rice emission estimate, and (c) rice emission estimate by Yan et al. (2009). The number of matching pairs is more than six for each grid for the twelve months from January to December.

where, VIS and NIR stand for the spectral reflectance measurements acquired in the visible (red) and near-infrared regions, respectively. It is a good indicator for assessing whether the target being observed contains live green vegetation or not (Tucker, 1979), though, quantitative interpretation may be difficult. We used the products derived by the Goddard earth sciences, data and information services center (GES

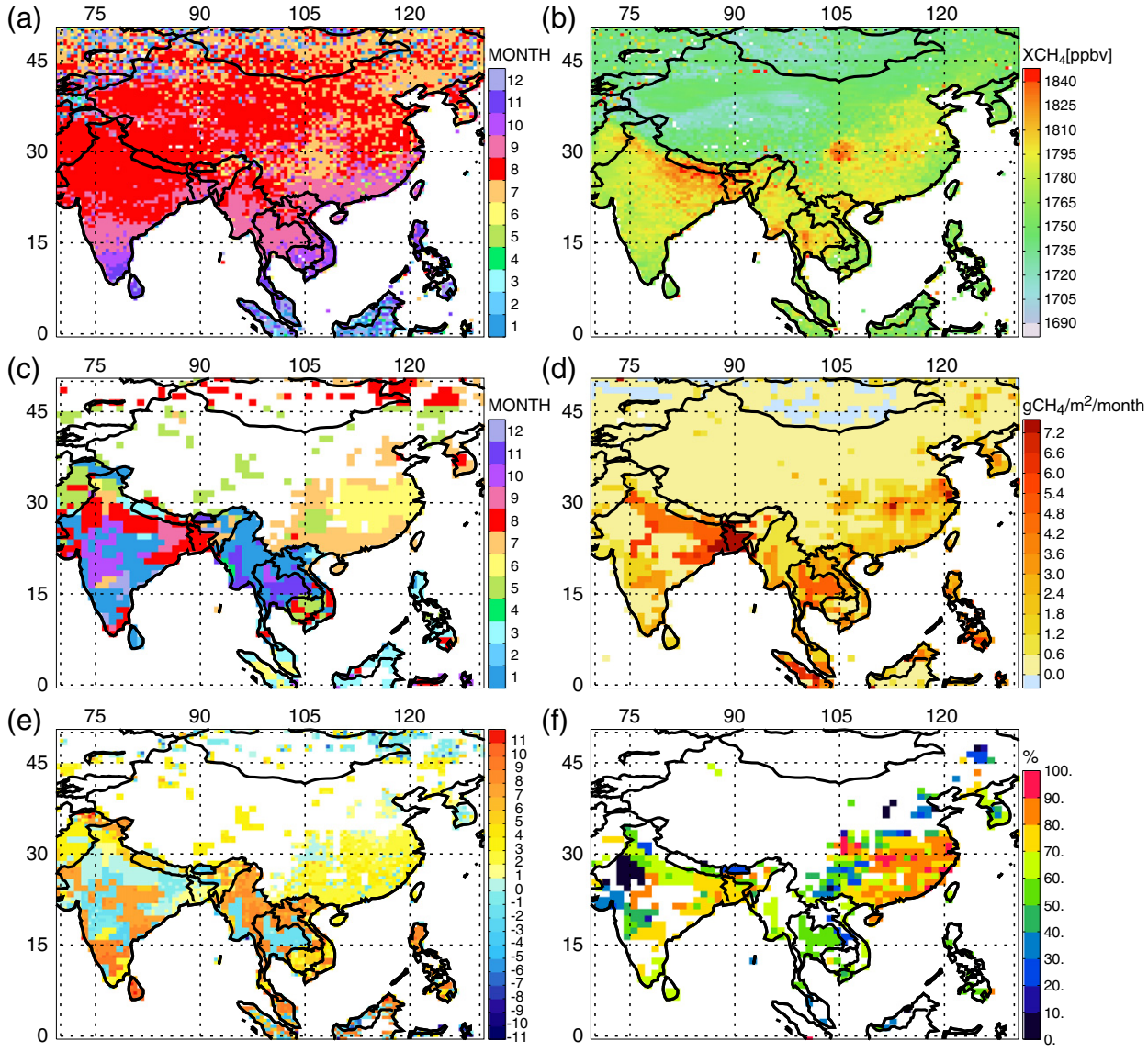

Fig. 6. *Top from left:* (a) The month in which xCH_4 reaches a maximum in each grid (0.5 × 0.5°) on a monthly basis. (b) Maximum value of xCH_4 on a monthly basis corresponding to the month shown in (a). *Middle from left:* (c) The month in which the GISS total CH_4 emission flux reaches a maximum in each grid (1.0° × 1.0°) on a monthly basis. (d) Maximum value of CH_4 emission flux on a monthly basis corresponding to the month shown in (c). *Bottom from left:* (e) Difference in months between the maximum of xCH_4 and GISS emission data, i.e., the difference of panels a and b. (f) Fraction of rice emission among all categories in GISS database. See text in Section 4 for more details on GISS.

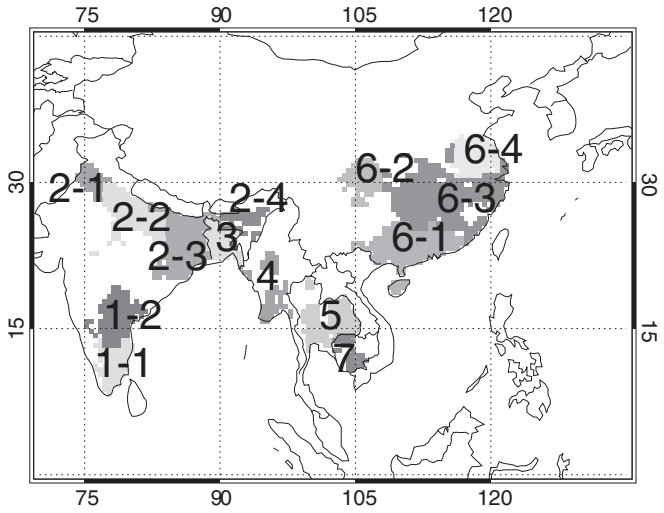

Fig. 7. Areas where CH_4 emission values are higher than 1.5 g CH_4 per year/m^2. The sampled areas, marked as Areas 1–7, are in South India, North India, Bangladesh, Myanmar, Thailand, China, and Cambodia. Table 3 presents the sub-regions.

Table 3
Summary of areas.

Code	Name	Sub-areas
1	South India	1-1, 1-2
2	North India	2-1, 2-2, 2-3, 2-4
3	Bangladesh	
4	Myanmar	
5	Thailand	
6	China	6-1, 6-2, 6-3, 6-4
7	Cambodia	

DISC) Northern Eurasian earth science partnership initiative project, with a resolution of 1° × 1° in latitude and longitude and archived the data on a monthly basis (Huete et al., 2002).

4. Emission inventory data

For comparing the satellite-derived indices mentioned above, bottom–up emission inventory data from Asia were taken from the GISS (Matthews et al., 1991). The data include emissions from 15 categories, of which, 6 categories (rice, wetlands, bogs, swamps, tundra, and biomass burning) are given as monthly estimates, since they exhibit significant seasonal variation. On the other hand, the other 9 categories such as ruminant animals, termites, pipelines, and so on, are considered to have constant values throughout the year.

In this study, we assumed the emission data, such as ruminant animals or pipelines, to have a constant value throughout the year. We thus divided the values by 12 to get a monthly-averaged value for each of the category. The monthly-averaged values for these categories were summed up with the data that show seasonality, such as rice paddies and wetlands. In this way, we rearranged the emission data for each month of the year, and 12-month data were compared with the xCH_4 measurements. We also used another emission data set obtained from YAN2009, whose estimate is much lower than that of the GISS database. Details of the emission data sets are summarized in Table 2.

5. Results and discussion

5.1. Distribution and seasonal variation of methane concentration and other indices

Fig. 2 shows the distribution of CH_4 concentration and other satellite-based indices over the Monsoon Asia. The SCIAMACHY xCH_4 and all other indices were averaged for 3 months to smooth out sporadic fluctuations and to enable the examination of seasonal variations. The first and second columns (December, January, February: DJF; and March, April, May: MAM) correspond to the "dry season" and the third and fourth columns (June, July, August: JJA; and September, October, November: SON) correspond to the "wet season" in Monsoon Asia. Fig. 2b and c shows LSWC and NDVI, respectively. The LSWC shows noticeable enhancement particularly during the wet season.

The seasonal variation of CH_4 concentration indicated in Fig. 2a is very different from that observed over the background regions such as over the Mauna Loa observatory (MLO) in the Pacific Ocean. From the monitoring network data, it is evident that over such background regions, CH_4 concentrations are generally lowest in summer and highest in winter (as in Fig. 4.4 of the WDCGG report, No. 36, WMO, 2012), because the rate of chemical loss reaction with OH is faster in summer. On the contrary, the seasonality of CH_4 concentration (Fig. 2a) over Monsoon Asia is characterized by higher values in the wet season (JJA and SON) and lower values in the dry season (DJF and MAM), possibly because of the effects of strong emissions from rice paddies and wetlands during the wet season. The NDVI (Fig. 2c) is also enhanced in JJA, following the increase in LSWC. In SON, the NDVI remains high, whereas, the LSWC somewhat decreases. Enhancement of the CH_4 concentration continues in SON in most of the regions where CH_4 is high in JJA.

In Fig. 3, the seasonal characteristics of CH_4 concentration are shown in terms of the Pearson's correlation coefficients (noted as r, hereafter) with LSWC and NDVI. The correlation coefficients shown in the figure were calculated for the twelve monthly-averaged values, each of which was averaged during the 6 years from January 2003 to December 2008. The data for the grids, where more than 6 pairs could be taken are selected and shown in the figure. Fig. 3a and b indicates the maps of the correlation coefficients between xCH_4 and LSWC (Fig. 3a), and between xCH_4 and NDVI (Fig. 3b). The r-values of xCH_4 and NDVI are considerably high in most of the regions examined here. The r-values for LSWC are not as high as that of NDVI; yet, this coefficient is greater than 0.6 in India and across most of Southeast Asia. Fig. 3c indicates distribution of the r-values for a limited period from May to December (8 months), which presents much higher "r" in Northern India, where double cropping of rice and wheat is practiced. This would be discussed in more detail in Section 5.2.

Emission inventory data have been mapped in Fig. 4 for comparison with the CH_4 distribution. Fig. 4a presents the GISS emission data that represents the total of all categories of the CH_4 emission sources, while only the rice emission estimate is shown in Fig. 4b. YAN2009 estimate from rice cultivation is also indicated in Fig. 4c. The geographical distribution of high CH_4 values in Fig. 2a corresponds to the strong emission regions indicated in the inventory maps (Fig. 4).

Fig. 5 shows the maps of r-values between xCH_4 (Fig. 2a) and each of the emission inventory data sets. Each of the panels in Fig. 5(a–c) corresponds to each of the data sets shown in Fig. 4. High correlation coefficients between xCH_4 and rice emission are indicated in Fig. 5, which proves a strong connection between enhancement of atmospheric CH_4 concentration and the emission of CH_4 from rice cultivation.

As the entire region of Monsoon Asia covers a wide range of climate zones and includes different phases of seasonal variation, the synoptic maps shown in Fig. 2a indicate composites of the various phases of different seasonal variations, and thus, it is difficult to distinguish the local maximum at a glance. To better understand the seasonal variation of CH_4 distribution, we focus on the month when the xCH_4 takes the maximum

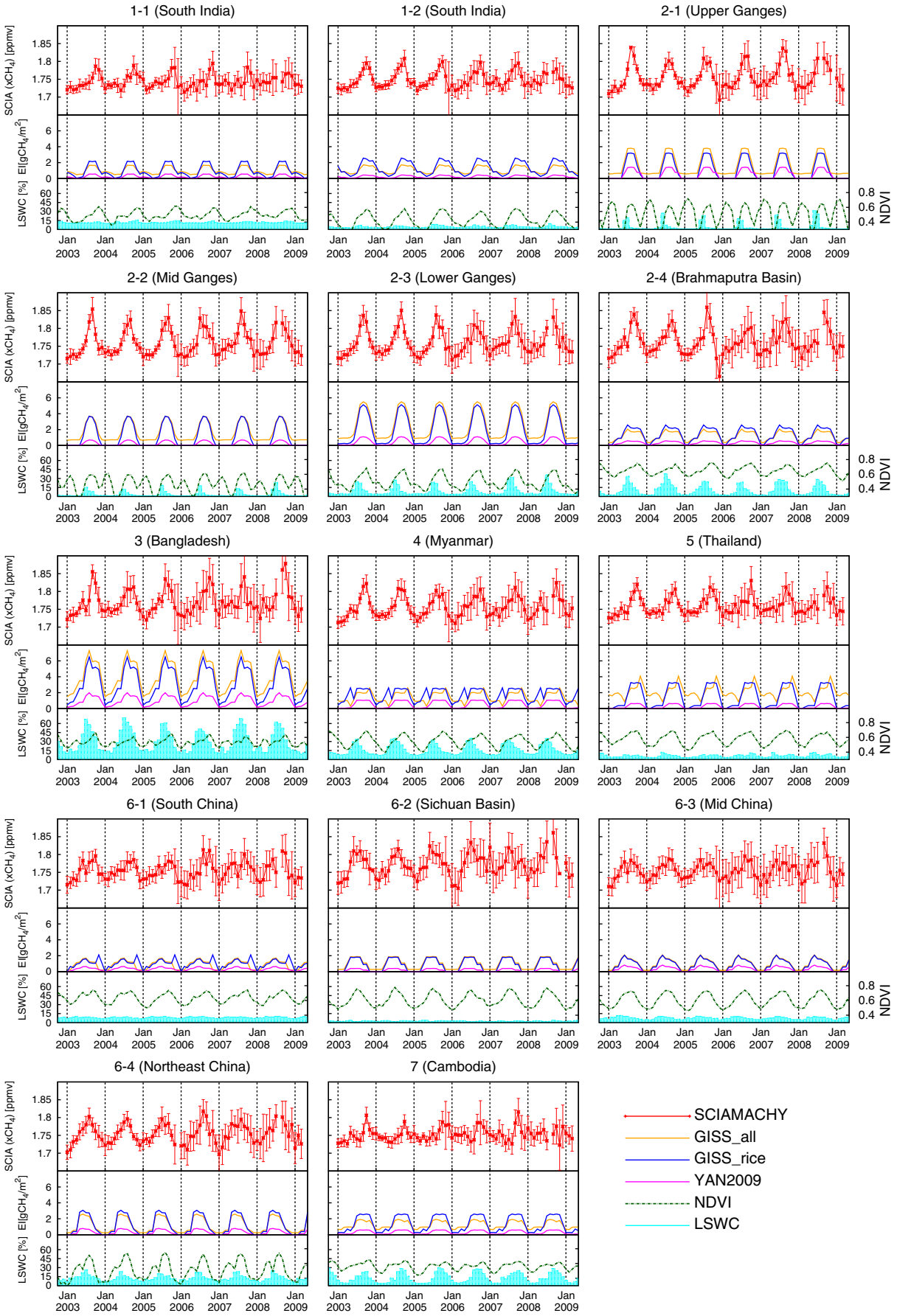
1-1 (South India)
1-2 (South India)
2-1 (Upper Ganges)
2-2 (Mid Ganges)
2-3 (Lower Ganges)
2-4 (Brahmaputra Basin)
3 (Bangladesh)
4 (Myanmar)
5 (Thailand)
6-1 (South China)
6-2 (Sichuan Basin)
6-3 (Mid China)
6-4 (Northeast China)
7 (Cambodia)
SCIA (xCH4) [ppmv]
EI[gCH4/m2]
LSWC [%]
NDVI
Jan 2003
Jan 2004
Jan 2005
Jan 2006
Jan 2007
Jan 2008
Jan 2009
SCIAMACHY
GISS_all
GISS_rice
YAN2009
NDVI
LSWC

value. Fig. 6a shows the months when xCH_4 was maximal on a monthly basis. The corresponding xCH_4 values at maximum are shown in Fig. 6b. Methane concentration was clearly enhanced over the Ganges Basin in North India and Bangladesh, the Chao Phraya Basin in Thailand, and the Sichuan Basin in China, suggesting strong CH_4 emissions around these areas at the peak month. The month of maximal xCH_4 basically depends on the latitude that also corresponds to a climate zone.

To examine the factors leading to the geographical patterns of seasonal variation in CH_4, the emission fluxes by GISS have also been analyzed in a similar way. We rearranged the data set into a monthly basis for comparison with the observed data, as described in Section 3. Fig. 6c and d depicts the results of a similar analysis to those in Fig. 6a and b, except the emission estimates. Note that there is no seasonal variation for some categories in the GISS emission database, as mentioned in Section 2. Therefore, the month of the maximum cannot be determined in some areas (white areas in Fig. 6c). The geographical pattern of the observed maximum value of CH_4 concentration (Fig. 6b) is similar to the estimated emission maximum, as in Fig. 6d. The similarity suggests that enhancement of CH_4 concentration over the region would mainly be controlled by CH_4 emissions, though transport should also play an important role and thus be considered.

We have also evaluated the time lag in the local maximum of the atmospheric CH_4 concentration and that of local emissions. Fig. 6e indicates the difference in months between the maximum of xCH_4 and GISS emission data, i.e., the difference of Fig. 6a and b. Positive values in Fig. 6e indicate that the month of xCH_4 maximum is earlier than the local emission maximum and vice versa. Fig. 6f presents the fraction of rice emission among all categories in GISS database. The fraction values are high (>50%) over the Ganges Basin, the Chao Phraya Basin, and the Ayeyarwady Basin. When Fig. 6e is compared with Fig. 6f, the xCH_4 maximum was observed after the local emission maximum. Therefore, the enhancement of atmospheric CH_4 could be interpreted as the result of emissions over those areas. We will discuss those typical rice paddy fields in the next section in more detail.

5.2. Detailed analysis of CH_4 concentration over rice paddies

As shown in Fig. 6f, in some parts of Monsoon Asia, rice emission is most significant among the emission categories. To examine the seasonal variation over such typical rice fields in more detail, we selected typical rice fields by sampling the regions where the CH_4 emission values from rice cultivation were estimated to be higher than 1.5 g CH_4/m^2/yr based on YAN2009's estimates. The sampled areas (Areas 1–7 in Fig. 7) represent South India, North India, Bangladesh, Myanmar, Thailand, China, and Cambodia, respectively. All of these areas are well known as major rice cultivation areas.

Some of the sampled areas include several sub-regions with different seasonal variations because of the different rice cultivation methods (e.g., two rice crops a year, double cropping with wheat). Hence, the sampled areas were divided into sub-areas, each of which has similar seasonal variation according to the emission inventory data. Using the statistical tool R (R Core Team, 2012) all the grid areas numbered 1, 2, and 6, were grouped into clusters, which are marked as 1-1, 1-2, and so on. The area codes are summarized in Table 3. In Vietnam, there are some areas where the CH_4 emission estimate is beyond the threshold. However, those areas are distributed in northern and southern parts of Vietnam separately, and each of the areas belongs to a different climate zone. We tried to separate those areas into several sub-areas, but the number of the data was not sufficient to keep statistical reliability for each area. Hence, we have excluded Vietnam in this study.

In the top panel of Fig. 8, the time series of SCIAMACHY xCH_4 from January 2003 to March 2009 over all of the areas shown in Fig. 7 are indicated. Each of the area code on the top of the panel is corresponding to Table 3. In the middle panel of the figure, the emission flux estimates taken from the GISS data set (GISS_all and GISS_rice) and YAN2009 are shown. Though these emissions are estimated for a fixed year and are not provided as year-by-year, the time series are drawn for all the years repeatedly. The LSWC and NDVI are also shown in the bottom panel. All of those data are integrated/averaged for individual area.

Fig. 9 shows the year-to-year variability of the correlation coefficients between xCH_4 and the parameters shown in Fig. 8, such as the emission inventory data sets, NDVI, and LSWC. As the fraction of rice emissions is large over those areas as shown in Fig. 6f, GISS_all is close to GISS_rice. YAN2009 is much lower than GISS_rice, but almost proportional. Therefore, the correlation coefficients for the three categories are often similar.

In most of the areas shown in Fig. 8, seasonal variations of CH_4 in the top panels show the maximum in summer monsoon season. In particular, the seasonal variation of xCH_4 is distinct in Northern India (Area 2), corresponding to the September maximum with relatively large amplitude (>1.0 ppmv). Over the Ganges Basin, the correlation coefficients between xCH_4 and the rice emission estimates are larger than 0.8 (see Areas 2-1, 2-2, and 2-3 in Fig. 9), suggesting strong direct connection between enhancement of CH_4 concentration and emission from the area. In Myanmar (Area 4), and Thailand (Area 5), the correlation between xCH_4 and rice emission estimate is also high ($r \gtrsim 0.6$), which can also be confirmed from Fig. 5. In general, the correlation coefficients between xCH_4 and rice emissions in China are relatively smaller than those in Southeast Asia, but some variations may occur depending on sub-areas.

Clear double peaks are the characteristic feature of NDVI in Area 2-1 and Area 2-2, reflecting double cropping (rice in summer and wheat in winter). On the other hand, in the lower reaches of the Ganges River (Area 2-3), the NDVI showed complicated seasonal variation suggesting that some one-crop and double-crop areas could be mixed. The correlation between xCH_4 and NDVI is generally large, $\gtrsim 0.6$ over most part of Monsoon Asia (see Fig. 3). However, the correlation is weak in Areas 2-1 and 2-2, as the NDVI has double peak corresponding to wheat and rice cultivation. Then, the correlation coefficient was recalculated for the limited period of summer monsoon season corresponding to rice cultivation (from May to November only); the recalculated result is shown as dashed lines in the panel of Areas 2-1 and 2-2 (see Fig. 3c as well). It is clear that the correlation coefficient of xCH_4 and NDVI in North India is higher in summer monsoon season (rice cultivation season) compared to the rest of the year. This suggests that the enhancement of CH_4 concentration is significantly caused by the rice cultivation in this region.

The correlation coefficient with LSWC is not as high as observed with NDVI. However, the correlation is generally moderate ($r > 0.5$) over rice paddy fields shown in Fig. 8, except for Sichuan Basin (Area 6-2), where the correlation is negative. The LSWC is generally low and constant throughout the year in this area. However, CH_4 emissions are estimated to be very high. As Fig. 6b shows, Sichuan Basin exhibits a distinctly high concentration of CH_4. The less amount of LSWC than other rice paddy areas is not well understood at present, and we need to investigate this further.

The time series of xCH_4 over Area 7 (Cambodia) do not show any regular seasonal variation as in other regions. However, the correlation of xCH_4 with emissions is larger than 0.4 except in the year 2008. The reason for the correlation with all parameters to be significantly lower in 2008 is under investigation.

Fig. 8. The area code is indicated at the top of each panel. *Upper row:* (red) Time series of monthly means of SCIAMACHY xCH_4 with standard deviation for each month. *Middle row:* Time series of emissions taken from the database of the GISS from all categories (GISS_all: orange) and from rice cultivation (GISS_rice: navy) (Matthews et al., 1991). Another rice emission taken from Yan et al. (2009) (YAN2009: purple) is also shown. Although these emissions are estimated for a fixed year, the time series are drawn for all years repeatedly. *Lower row:* Time series of NDVI (lines in green) and LSWC (bars in light blue).

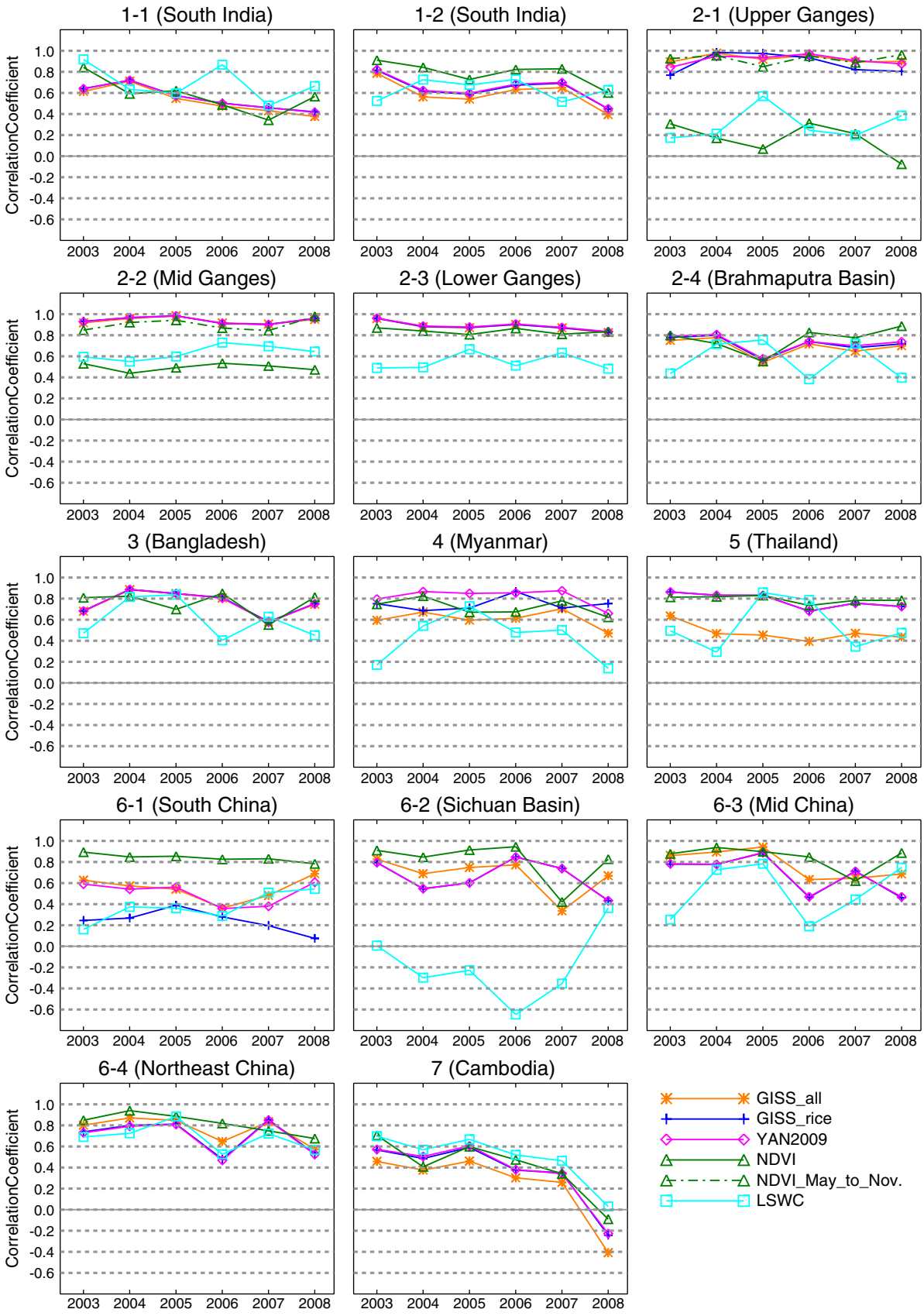

Fig. 9. Year to year variability of the Pearson's correlation coefficients between SCIAMACHY xCH_4 and the GISS from all categories (GISS_all: orange), GISS from rice cultivation (GISS_rice: navy), rice emission taken from Yan et al. (2009) (YAN2009: purple), NDVI (green), and LSWC (light blue). Each panel is corresponding to the areas shown in Table 3 as in Fig. 8. In Areas 2-1 and 2-2, the correlation coefficients calculated for the period from May to December are also shown for NDVI as dashed lines.

5.3. Discussion of uncertainties

In North India, the geographical distribution of xCH_4 enhancement is very closely correlated with the rice emission; thus, we expect the xCH_4 enhancement to be due to strong emissions from this area. However, the SCIAMACHY measurement represents the column average xCH_4 values, as described in Section 2; and thus, the variation of xCH_4 cannot be directly interpreted as the variation of CH_4 concentration at the surface. Therefore, we should carefully examine the attributes that cause enhancement of xCH_4. If the enhancement of xCH_4 were x ppmv in the boundary layer with thickness of up to 800 hPa (~2 km in altitude), the enhancement of the column average, xCH_4, would be about 0.2x ppmv. This is because the air mass below 800 hPa is about 20% of the total column of the air. As the amplitude of seasonal variation of xCH_4 over North India is approximately 0.14 ppmv (see Fig. 8), the enhancement of 0.7 ppmv in the boundary layer could explain the enhancements of xCH_4, because 0.14 ppmv/0.2 = 0.7 ppmv. We analyzed the air samples taken over rice paddies near Karnal in Haryana and near Ganges in Varanasi in the month of August 2012 and found the surface CH_4 concentrations over rice paddies to be more than 2 ppmv, and at some instances, even more than 2.2 ppmv (note that the global background is ~1.7 ppmv). Even though the measurements are preliminary in nature and the results are still under examination, these numbers are sufficiently consistent to indicate the effect of emissions on the enhancement of xCH_4. Long term sampling at regular intervals in the Northern India could generate more reliable interpretation in the near future.

Transport is another important issue to be considered. As indicated by Randel et al. (2010), convection of the atmosphere over Tibetan Plateau should play an important role in the transport of CH_4 from the ground up to mid- or upper-troposphere. There have been some reports of CH_4 plumes being observed in the upper troposphere over India (Baker et al., 2012; Xiong et al., 2009). To interpret the enhancement of xCH_4, we also need to consider the possibility of CH_4 enhancement in the upper troposphere. This is because the average of the column amount can be affected by the CH_4 enhancement in the upper atmosphere. However, the measurements from the TIR sensors or airplane measurements during level flight (not during ascent or descent) cannot provide any information at altitudes lower than ~2 km, which is a region more sensitive to emissions from the ground. Though it is not possible to detect vertical profile only from SWIR sensors, it would be possible to subtract the CH_4 amount in the lower troposphere by the combined use of SWIR and TIR sensors. This challenging task will be taken up in our future studies.

In this study, we have not applied any atmospheric transport model, though we are already preparing to use one. However, we can demonstrate that, at least, some areas such as the Ganges Basin or Sichuan Basin are definitely strong emission areas as shown in Fig. 6b that indicates the maximum value of the year. Even if the transport processes have strong effects on the CH_4 distribution, it could not be possible for any area to appear as a hotspot without strong emission from the area. When comparing Fig. 6b and d, it is observed that the Sichuan Basin has a high concentration of CH_4. Bergamaschi et al. (2009) had already reported that the enhancement there was noticeable throughout the year having the maximum value in Asia. They inferred that such high values may be due to the intense rice cultivation and the possibility of gas pipelines. However, this inference remains a speculation; the reason of high concentration in Sichuan Basin is not yet fully understood. To the extent that we surveyed local people, no concrete evidence showing pipeline leakage was found. This is an important area we intend to investigate in the near future.

We should note that the high correlation between CH_4 concentration and NDVI need not necessarily indicate a cause and effect relationship. However, as shown in Fig. 8, the high r-vales over rice paddies, approximately unity in some areas, would suggest the relationship between rice growth and CH_4 emissions to some extent. In Southeast Asia, r-values with GISS_all are not as high as with GISS_rice or YAN2009, which implies the relatively greater importance of rice emissions among other emission categories in this region.

6. Concluding remarks

In this study, we showed the characteristics of CH_4 distribution in Monsoon Asia. We also compared the column-averaged CH_4 concentration (xCH_4) obtained using the satellite sensor, SCIAMACHY, with the bottom–up emission inventory data sets and the satellite-derived indices such as the LSWC and the NDVI.

The seasonality of xCH_4 observed by SCIAMACHY (shown Fig. 2a) is characterized by high values particularly during the wet seasons. The geographical distribution of high CH_4 values in Fig. 2a corresponds to the strong emission regions indicated in the inventory maps shown in Fig. 4. High correlation coefficients (r) between xCH_4 and rice emission estimate is indicated in Fig. 5, which suggests the strong connection between the atmospheric CH_4 concentration and the CH_4 emissions from rice cultivation for most of the areas in Monsoon Asia. When focusing on typical rice paddies, strong relationship between xCH_4 enhancement and rice emission estimate is outstanding (as shown in Figs. 8 and 9). In Southeast Asia, r-values with rice emission are high, suggesting the relative importance of rice emission among other emission categories in the area.

The seasonality of NDVI is similar to xCH_4; NDVI is high during the wet season and low in the dry season. The correlation between xCH_4 and NDVI is considerably strong in most of the regions examined in this study. The r-values for LSWC are not as high as for NDVI ($r > 0.6$) in most of the regions examined in this study.

The results obtained in this study demonstrate the potential of satellite observation at short-wavelength infrared (SWIR). The atmospheric CH_4 measurements by SWIR sensor have enough information for detecting emissions from the ground, though it can provide reliable information only for the column-averaged concentration.

Acknowledgments

We express our gratitude to Ms. H. Araki for her help with data analysis and drawing figures. This study was supported by a Grant-in-Aid from the Green Network of Excellence, Environmental Information (GRENE-ei) program. This research was also supported by the Environment Research and Technology Development Fund of the Ministry of the Environment, Japan (A1202). Finally, we wish to thank the three anonymous reviewers for their valuable suggestions that have improved this manuscript significantly.

References

Baker, A. K., Schuck, T. J., Brenninkmeijer, C. A.M., Rauthe-Schöch, A., Slemr, F., van Velthoven, P. F. J., et al. (2012). Estimating the contribution of monsoon-related biogenic production to methane emissions from South Asia using CARIBIC observations. *Geophysical Research Letters, 39*, 1–6.

Bergamaschi, P., Frankenberg, C., Meirink, J. F., Krol, M., Villani, M. G., Houweling, S., et al. (2009). Inverse modeling of global and regional CH_4 emissions using SCIAMACHY satellite retrievals. *Journal of Geophysical Research, 114*, http://dx.doi.org/10.1029/2009JD012287.

Bovensmann, H., Burrows, J. P., Buchwitz, M., Frerick, J., Noel, S., & Rozanov, V. V. (1999). SCIAMACHY: Mission Objectives and Measurement Modes. *Journal of the Atmospheric Sciences, 56*, 127–150.

Cicerone, R. J., & Shetter, J.D. (1981). Sources of atmospheric methane: Measurements in rice paddies and discussion. *Journal of Geophysical Research, 86*, 7203–7209.

Denman, K. L., Brasseur, G., Chidthaisong, A., Ciais, P., Cox, P.M., Dickinson, R. E., et al. (2007). Couplings between changes in the climate system and biogeochemistry, Climate Change 2007: The Physical Science Basis. *Contribution of Working Group I to the Fourth Assessment Report of the Intergovernmental Panel on Climate Change: The Physical Science Basis. Contribution of Working Group I to the Fourth Assessment Report of the Intergovernmental Panel on Climate Change*.

Dlugokencky, E. J., Bruhwiler, L. M. P., White, J. W. C., Emmons, L. K., Novelli, Paul C., Montzka, Stephen A., et al. (2009a). Observational constraints on recent increases in the atmospheric CH_4 burden. *Geophysical Research Letters, 36*, L18803, http://dx.doi.org/10.1029/2009GL039780.

Dlugokencky, E. J., Lang, P.M., & Masarie, K. A. (2009b). *Atmospheric Methane Dry Air Mole Fractions from the NOAA ESRL Carbon Cycle Cooperative Global Air Sampling Network, 1983–2008, Version: 2009-06-18.* (ftp. *ftp.cmdl.noaa.gov/ccg/ch4/flask/event*).

Dlugokencky, E. J., Nisbet, E. G., Fisher, R., & Lowry, D. (2011). Global atmospheric methane: Budget, changes and dangers. *Philosophical Transactions. Series A, Mathematical, Physical, and Engineering Sciences*, *369*, 2058–2072.

FAO (2013). FAOSTAT. http://faostat3.fao.org/home/index.html#DOWNLOAD

Forster, P., Ramaswamy, V., Artaxo, P., Berntsen, T., Betts, R., Fahey, D. W., et al. (2007). Changes in atmospheric constituents and in radiative forcing. *Climate Change 2007*. Cambridge, United Kingdom and New York, NY, USA: Cambridge University Press.

Frankenberg, C., Aben, I., Bergamaschi, P., Dlugokencky, E. J., van Hees, R., Houweling, S., et al. (2011). Global column-averaged methane mixing ratios from 2003 to 2009 as derived from SCIAMACHY: Trends and variability. *Journal of Geophysical Research*, *116*, http://dx.doi.org/10.1029/2010JD014849.

Frankenberg, C., Bergamaschi, P., Butz, A., Houweling, S., Meirink, J. F., Notholt, J., et al. (2008). Tropical methane emissions: A revised view from SCIAMACHY onboard ENVISAT. *Geophysical Research Letters*, *35*, http://dx.doi.org/10.1029/2008GL034300.

Frankenberg, C., Meirink, J. F., Bergamaschi, P., Goede, A. P. H., Heimann, M., Körner, S., et al. (2006). Satellite chartography of atmospheric methane from SCIAMACHY on board ENVISAT: Analysis of the years 2003 and 2004. *Journal of Geophysical Research*, *111*, http://dx.doi.org/10.1029/2005JD006235.

Frankenberg, C., Meirink, J. F., van Weele, M., Platt, U., & Wagner, T. (2005). Assessing methane emissions from global space-borne observations. *Science*, *308*, 1010–1014.

Huete, A., Didan, K., Miura, T., Rodriguez, E. P., Gao, X., & Ferreira, L. G. (2002). Overview of radiometric and biophysical performance of the MODIS vegetation indices. *Remote Sensing of Environment*, *83*, 195–213.

Intergovernmental Panel on Climate Change (IPCC) (1994). Radioactive forcing of climate change and an evaluation of the IPCC IS92 emission scenarios. In J. T. Houghton (Ed.), *Climate Change 1994*. Cambridge, U. K.: Cambridge Univ. Press.

Intergovernmental Panel on Climate Change (IPCC) (2007). *2006 IPCC Guidelines for National Greenhouse Gas Inventories*. Hayama, Japan: Inst. for Global Environ. Strategies.

Matthews, E., Fung, I., & Lerner, J. (1991). Methane emission from rice cultivation: Geographic and seasonal distribution of cultivated areas and emissions. *Global Biogeochemical Cycles*, *5*, 3–24.

Peters, W., Jacobson, A.R., Sweeney, C., Andrews, A. E., Conway, T. J., Masarie, K., et al. (2007). An atmospheric perspective on North American carbon dioxide exchange: CarbonTracker. *Proceedings of the National Academy of Sciences of the United States of America*, *104*, 18925–18930.

R: A language, environment for statistical computing (2012). Vienna, Austria: R Foundation for Statistical Computing (http://www.r-project.org).

Randel, W. J., Park, M., Emmons, L., Kinnison, D., Bernath, P., Walker, K. A., et al. (2010). Asian monsoon transport of pollution to the stratosphere. *Science*, *328*, 611–613.

Sass, R. L., & Cicerone, R. J. (2002). Photosynthate allocations in rice plants: Food production or atmospheric methane? *Proceedings of the National Academy of Sciences of the United States of America*, *99*, 11993–11995.

Seiler, W., Holzapfel-Pschorn, A., Conrad, R., & Scharffe, D. (1984). Methane emission from rice paddies. *Journal of Atmospheric Chemistry*, *1*, 241–268.

Sheshakumar, K. G., Singh, R. P., Panigrahy, S., & Parihar, J. S. (2011). Analysis of seasonal variability of vegetation and methane concentration over India using SPOT-VEGETATION and ENVISAT-SCIAMACHY data. *Journal of the Indian Society of Remote Sensing*, *39*, 315–321.

Takeuchi, W., & Gonzalez, L. (2009). Blending MODIS and AMSR-E to predict daily land surface water coverage. *Proceedings of International Remote Sensing Symposium (ISRS), Busan, South Korea, 2009 Oct. 29*.

Tucker, C. J. (1979). Red and photographic infrared linear combinations for monitoring vegetation. *Remote Sensing of Environment*, *8*, 127–150.

WMO (2012). *WDCGG Data Report No. 36*.

Xiong, X., Howelling, S., Wei, J. C., Maddy, E., Sun, F., & Barnet, C. (2009). Methane plume over south Asia during the monsoon season: Satellite observation and model simulation. *Atmospheric Chemistry and Physics*, *9*, 783–794.

Yan, X., Akiyama, H., Yagi, K., & Akimoto, H. (2009). Global estimations of the inventory and mitigation potential of methane emissions from rice cultivation conducted using the 2006 Intergovernmental Panel on Climate Change Guidelines. *Global Biogeochemical Cycles*, *23*, http://dx.doi.org/10.1029/2008GB003299.